

Berezinskii-Kosterlitz-Thouless Phase Transition in 2D Spin-Orbit Coupled Fulde-Ferrell Superfluids

Yong Xu¹ and Chuanwei Zhang^{1*}

¹*Department of Physics, The University of Texas at Dallas, Richardson, Texas 75080, USA*

The experimental observation of traditional Zeeman-field induced Fulde-Ferrell-Larkin-Ovchinnikov (FFLO) superfluids has been hindered by various challenges, in particular, the requirement of low dimension systems. In 2D, it is well known that finite temperature phase fluctuations lead to extremely small Berezinskii-Kosterlitz-Thouless (BKT) transition temperature, raising serious concern regarding the observability of 2D FFLO superfluids. Recently, it was shown that FFLO superfluids can be realized using a Rashba spin-orbit coupled Fermi gas subject to Zeeman fields, which may also support topological excitations such as Majorana fermions in 2D. Here we address the finite temperature BKT transition issue in this system, which may exhibit gapped, gapless, topological, and gapless topological FF phases. We find a large BKT transition temperature due to large effective superfluid densities, making it possible to observe 2D FF superfluids at finite temperature. In addition, we show that gapless FF superfluids can be stable due to their positive superfluid densities. These findings pave the way for the experimental observation of 2D gapped and gapless FF superfluids and their associated topological excitations at finite temperature.

PACS numbers: 03.75.Ss, 03.75.Lm, 74.20.Fg

The exotic Fulde-Ferrell-Larkin-Ovchinnikov (FFLO) superfluids [1, 2] with finite center-of-mass momentum Cooper pairing have played a central role in various fields of physics, such as heavy-fermion superconductors [3–5], organic superconductors [6], two-dimensional electron gases [7], and cold Fermi gases [8]. Despite intensive search, no conclusive evidence of FFLO states has been experimentally observed. One challenge comes from the narrow region of the phase diagram where FFLO superfluids exist [9]. This region increases dramatically in lower dimensions [10, 11]. However, owing to thermal fluctuations, low dimensional systems cannot undergo conventional phase transition to a state with long-range order. In particular, in two dimension (2D), the relevant physics is the Berezinskii-Kosterlitz-Thouless (BKT) transition [12, 13] to a state with quasi-long-range order (*i.e.* vortex-antivortex (V-AV) pairs) [14–16], with the critical temperature T_{BKT} determined by the superfluid density tensor. However, in traditional Zeeman field induced FFLO states, the effective superfluid density for T_{BKT} is extremely small (even zero for FF states) due to the rotational symmetry of the Fermi surface [17, 18], raising a realistic question that whether FFLO states can indeed be observable in 2D at finite temperature.

In the past few years, synthetic spin-orbit coupling [19–25] has attracted increasing attention in cold atom community because of its key role in many intriguing physics such as topological superfluids [26–32], which can accommodate Majorana fermions in low dimension with potential applications in fault-tolerant topological quantum computation [33]. In a spin-orbit coupled Fermi gas with an in-plane Zeeman field, FF superfluids are dominant in the low temperature phase diagram due to the asymmetric Fermi surface [34–41]. Furthermore, topological FF superfluids were found with an additional out-of-

plane Zeeman field [42–49]. However, previous results are mainly based on mean-field theory, and it is natural to ask whether such FF superfluids can be observed experimentally at finite temperature in 2D through the BKT mechanism. In particular, these FF states exhibit gapless quasi-particle excitations in some parameter regions [35, 38, 46–49], whose stability becomes a serious issue, similar as the well known unstable breached pair (BP) phases with *s*-wave contact interactions due to the divergence of fluctuations [50–52].

In this Letter, we address these crucial issues by studying 2D spin-orbit coupled Fermi gases with both in-plane and out-of-plane Zeeman fields in the presence of finite temperature phase fluctuations beyond mean-field theory. Our main findings are that: 1) The finite momentum of Cooper pairs leads to anisotropic superfluid densities along the *x* and *y* directions. However, they are both nonzero and large, in contrast to zero transverse superfluid density in traditional Zeeman field induced FF superfluids. This leads to a finite BKT transition temperature, making it possible to observe FF superfluids in 2D. 2) The superfluid densities for gapless states including gapless FF and gapless topological FF superfluids are positive, implying gapless FF superfluids are stable, which are different from the unstable BP phase with a negative superfluid density. 3) The changes of T_{BKT} with respect to Zeeman fields exhibit an inflection point, where the gap of the quasi-particle excitation spectrum at zero momentum closes. In particular, this inflectional behavior is stronger for a gapless state because of the higher density of states. 4) The anisotropic superfluid density tensor leads to anisotropic V-AV pairs below the BKT temperature.

Consider a 2D Rashba-type spin-orbit coupled Fermi gas subject to both in-plane (h_x) and out-of-plane (h_z)

Zeeman fields and s-wave attractive contact interactions. The 2D system can be realized experimentally by a strong harmonic trap or deep optical lattices, which freeze atoms to the ground state along the third dimension. The many-body Hamiltonian reads

$$H = \int d\mathbf{r} \hat{\Psi}^\dagger(\mathbf{r}) H_s(\hat{\mathbf{p}}) \hat{\Psi}(\mathbf{r}) - U \int d\mathbf{r} \hat{\Psi}_\uparrow^\dagger(\mathbf{r}) \hat{\Psi}_\downarrow^\dagger(\mathbf{r}) \hat{\Psi}_\downarrow(\mathbf{r}) \hat{\Psi}_\uparrow(\mathbf{r}), \quad (1)$$

where the single particle Hamiltonian $H_s(\hat{\mathbf{p}}) = \frac{\hat{\mathbf{p}}^2}{2m} - \mu + H_{\text{SOC}}(\hat{\mathbf{p}}) + H_z$ with momentum operator $\hat{\mathbf{p}} = -i\hbar(\partial_x \mathbf{e}_x + \partial_y \mathbf{e}_y)$, chemical potential μ , attractive interaction strength U , and the atom mass m . The Rashba SO coupling $H_{\text{SOC}}(\hat{\mathbf{p}}) = \alpha(\hat{\mathbf{p}} \times \sigma) \cdot \mathbf{e}_z$ with Pauli matrix σ ; the Zeeman field $H_z = h_x \sigma_x + h_z \sigma_z$ along the x (in-plane) and z (out-of-plane) directions. $\hat{\Psi}(\mathbf{r}) = [\hat{\Psi}_\uparrow(\mathbf{r}), \hat{\Psi}_\downarrow(\mathbf{r})]^T$ and $\hat{\Psi}_\nu^\dagger(\mathbf{r})$ ($\hat{\Psi}_\nu(\mathbf{r})$) creates (annihilates) a fermionic atom at \mathbf{r} . In experiments, the SO coupling and Zeeman fields can be achieved by coupling two hyperfine states via Raman lasers for ultracold fermionic atoms [19–25].

The partition function at temperature $T = 1/\beta$ can be written as an imaginary time coherent path integral $Z = \text{Tr}(e^{-\beta H}) = \int D(\bar{\psi}, \psi) e^{-S[\bar{\psi}, \psi]}$ in quantum field theory, where the action $S[\bar{\psi}, \psi] = \int_0^\beta d\tau \left(\int d\mathbf{r} \sum_\sigma \bar{\psi}_\sigma \partial_\tau \psi_\sigma + H(\bar{\psi}, \psi) \right)$ with an imaginary time integral $\int d\tau$ and $H(\bar{\psi}, \psi)$ obtained by replacing $\hat{\Psi}_\sigma^\dagger$ and $\hat{\Psi}_\sigma$ with Grassman field number $\bar{\psi}_\sigma$ and ψ_σ respectively. Based on Hubbard-Stratonovich transformation, the fermion degree can be integrated out, leading to $Z = \int D(\bar{\Delta}, \Delta) e^{-S_{\text{eff}}[\bar{\Delta}, \Delta]}$ with the effective action written as

$$S_{\text{eff}}[\bar{\Delta}, \Delta] = \int_0^\beta d\tau \int d\mathbf{r} \frac{|\Delta|^2}{U} - \frac{1}{2} \ln \det G^{-1}, \quad (2)$$

where the inverse single particle Green function $G^{-1} = -\partial_\tau - H_B$ in the Nambu-Gorkov basis, with 4×4 Bogoliubov-de Gennes (BdG) Hamiltonian

$$H_B = \begin{pmatrix} H_s(\hat{\mathbf{p}}) & \Delta(\mathbf{r}, \tau) \\ \Delta(\mathbf{r}, \tau) & -\sigma_y H_s(\hat{\mathbf{p}})^* \sigma_y \end{pmatrix}. \quad (3)$$

By postulating $\Delta(\mathbf{r}) = \Delta_0 e^{iQ_y y}$ in terms of the broken symmetry of the Fermi surface along the y direction [41], the mean-field saddle point in the absence of phase fluctuations can be obtained by the saddle equations $\partial\Omega/\partial\Delta_0 = 0$, $\partial\Omega/\partial Q_y = 0$, and the particle number equation $\partial\Omega/\partial\mu = -n$ with a fixed total density n [46]. $\Omega = S_{\text{eff}}/\beta$ is the thermodynamical potential. Here the ultra-violet divergence can be regularized by $1/U = \sum_{\mathbf{k}} 1/(\hbar^2 k^2/m + E_b)$ with the binding energy E_b .

To study the effects of phase fluctuations, we set $\Delta(\mathbf{r}, \tau) = \Delta_0 e^{iQ_y y + i\theta(\mathbf{r}, \tau)}$, where $\theta(\mathbf{r}, \tau)$ is the phase fluctuations around the saddle point. The inverse Green function $G^{-1} = G_0^{-1} + \Sigma$ with the mean-field one

G_0^{-1} and self-energy $\Sigma = (i\partial_\tau \theta/2 + \hbar^2 Q_y \partial_y \theta/4m + \hbar^2 (\nabla \theta)^2/8m) \sigma_z \otimes \sigma_0 + \hbar \nabla \theta \cdot \hat{\mathbf{p}}/2m - i\hbar^2 \nabla^2 \theta/4m + \alpha \hbar \partial_x \theta/2(\sigma_0 \otimes \sigma_y) - \alpha \hbar \partial_y \theta/2(\sigma_0 \otimes \sigma_x)$. The effective action $S_{\text{eff}} = S_{\text{eff}}^0 + S_{\text{eff}}^{\text{fluc}}$ with the contribution of the fluctuations $S_{\text{eff}}^{\text{fluc}} = \text{tr} \sum_{n=1}^\infty (G_0 \Sigma)^n/2n$. Expanding it to the second order yields

$$S_{\text{eff}}^{\text{fluc}} = \frac{1}{2} \int_0^\beta d\tau \int d\mathbf{r} [J_{xx}(\partial_x \theta)^2 + J_{yy}(\partial_y \theta)^2 + J_{\tau y} i \partial_\tau \theta \partial_y \theta + P(\partial_\tau \theta)^2 - iA \partial_\tau \theta], \quad (4)$$

where $J_{\nu\mu}$ is the superfluid density tensor (here $J_{xy} = 0$) and the corresponding superfluid density $\rho_{\mu\nu} = 4m J_{xy}/(\hbar^2 n)$ scaled by the fixed total density; P is the compressibility. Compared to the formula for the normal BCS superfluids [16], one additional term $J_{\tau y}$ emerges because of the nonzero Cooper pairing momentum Q_y . Note that these parameters cannot be expressed analytically and they are obtained via numerical approach (See supplementary materials). We have checked that the results in the absence of h_x are exactly the same as previous results [16].

By decomposing the phase $\theta(\mathbf{r}, \tau)$ into two parts: a static vortex configuration $\theta(\mathbf{r})_v$ and a time-dependent spin-wave one $\theta(\mathbf{r}, \tau)_{sw}$, the effective action contributed by phase fluctuations can be written as $S_{\text{eff}}^{\text{fluc}} = S_{\text{eff}}^v + S_{\text{eff}}^{sw}$, where the vortex part $S_{\text{eff}}^v = \frac{1}{2} \int d\mathbf{r} \sum_{\nu=x,y} J_{\nu\nu} (\partial_\nu \theta_v)^2$ and spin-wave part $S_{\text{eff}}^{sw} = \frac{1}{2} \int d\mathbf{r} [\sum_{\nu=x,y} J_{\nu\nu} (\partial_\nu \theta_{sw})^2 + J_{\tau y} i \partial_\tau \theta \partial_y \theta_{sw} + P(\partial_\tau \theta_{sw})^2 - iA \partial_\tau \theta_{sw}]$. The integration of the spin-wave part gives $S_{\text{eff}}^{sw} = \sum_{\mathbf{k}} \ln(1 - e^{-\beta E_{sw}(\mathbf{k})})$ where the spin-wave excitation $E_{sw}(\mathbf{k}) = [-J_{\tau y} k_y + \sqrt{J_{\tau y}^2 k_y^2 + 4P(J_{xx} k_x^2 + J_{yy} k_y^2)}]/2P$. This anisotropic linear spectrum has anisotropic sound speeds: $v_x = \sqrt{J_{xx}/P}$, $v_{y+} = (-J_{\tau y} + \sqrt{J_{\tau y}^2 + 4PJ_{yy}})/2P$, and $v_{y-} = (J_{\tau y} + \sqrt{J_{\tau y}^2 + 4PJ_{yy}})/2P$ along the x direction, positive and negative y directions [46]. We note that anisotropic sound speed also exists in other anisotropic systems [53], whereas the anisotropic behavior along the same direction can occur only in a FF superfluid. In a normal BCS superfluid, $Q_y = 0$ and $v = \sqrt{J_{xx}/P}$ [14, 16].

In the presence of phase fluctuations, the parameters Δ_0 , Q_y , and μ can be calculated by self-consistently solving the saddle equations $\partial\Omega^0/\partial\Delta_0 = 0$, $\partial\Omega/\partial Q_y = 0$, and the particle number equation $\partial\Omega/\partial\mu = -n$, where $\Omega^0 = S_{\text{eff}}^0/\beta$ and $\Omega = S_{\text{eff}}/\beta$. Instead of the critical temperature determined by $\Delta_0 = 0$ in the mean-field theory, the critical BKT temperature is determined [13, 18, 53] (See supplementary materials) by

$$T_{\text{BKT}} = \frac{\pi}{2} J(\Delta_0, Q_y, \mu, T_{\text{BKT}}), \quad (5)$$

with $J = \sqrt{J_{xx} J_{yy}}$ that generally does not vanish at T_{BKT} . Across T_{BKT} that is much lower than the mean-field critical temperature, Fermi gases transit from a

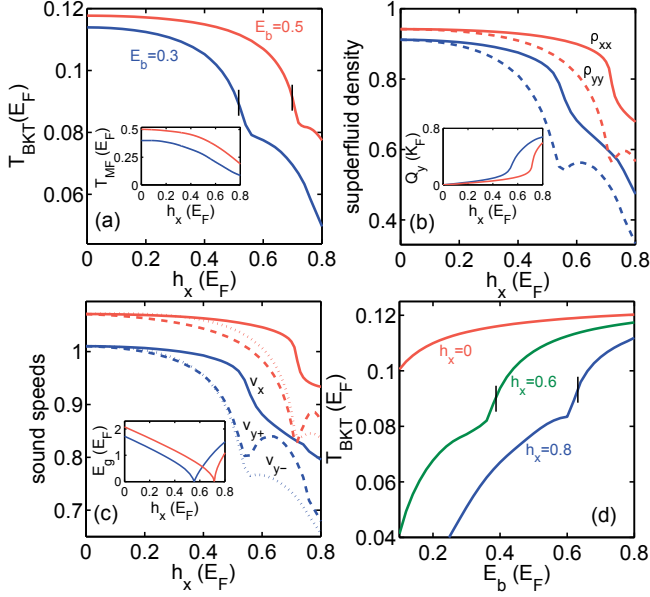


FIG. 1: (Color online) Plot of T_{BKT} (in (a)), superfluid densities and sound speeds (in (b) and (c)) evaluated at T_{BKT} , as a function of h_x with $E_b = 0.3E_F$ and $E_b = 0.5E_F$. The transition from gapped to gapless superfluids is marked by a short vertical line. In the inset of (a), (b), and (c), the mean-field critical temperatures, the momentum of Cooper pairs Q_y at T_{BKT} , and the gap at zero momentum at T_{BKT} are plotted respectively. The unit of the speed of sounds is $v_F/\sqrt{2}$ with Fermi velocity v_F and the unit of superfluid densities is n . In (b), the solid and dashed lines correspond to ρ_{xx} and ρ_{yy} respectively. In (c) and (d), the solid, dashed, and dotted lines respectively correspond to the sound speeds along the x direction v_x , along positive y direction v_{y+} , and negative y direction v_{y-} . (d) Plot of T_{BKT} with respect to the binding energy E_b at fixed h_x . Here $\alpha K_F = E_F$ and $h_z = 0$.

pseudogap phase (with nonzero Δ_0 but without phase coherence) to a superfluid affluent with V-AV pairs (with both pairing and phase coherence). T_{BKT} can be obtained by performing self-consistent calculation of the saddle point equations, the particle number equation, and Eq.(5). The energy unit is chosen as the Fermi energy $E_F = \hbar^2 \mathbf{K}_F^2 / 2m$ of non-interacting Fermi gases without SO coupling and Zeeman fields with Fermi vector $K_F = (3\pi^2 n)^{1/3}$.

The BKT phase transition for FF states was studied for imbalanced Fermi gases without spin-orbit coupling and it was found that the superfluid density in the direction perpendicular to the finite momenta of Cooper pairs is zero due to the rotational invariance of the Fermi surface [17, 18], suggesting that FF superfluids may not be observable at finite temperature in 2D. Even considering the LO state, the critical temperature is still much lower because of the extremely high anisotropy of the superfluid density [17]. However, in Fig. 1, we find that the BKT critical temperature T_{BKT} for the FF superfluids is finite and large. Although the superfluid densities are

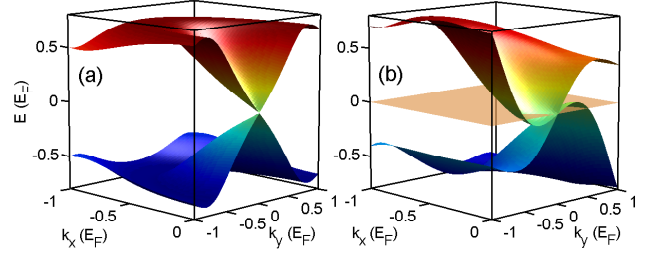


FIG. 2: (Color online) Quasi-particle excitations in the (k_x, k_y) plane at the critical point (a) from normal superfluids to topological superfluids, where $h_x = 0$ and $h_z = 0.652E_F$; and (b) from gapless FF superfluids to gapless topological FF superfluids, where $h_x = 0.5$ and $h_z = 0.282$. The physical quantities are evaluated at T_{BKT} . The light color plane in (b) corresponds to zero excitation energy. Here $\alpha K_F = E_F$ and $E_b = 0.3E_F$.

still anisotropic, this anisotropy is not high enough to destroy the superfluidity at finite temperature. This result provides the theoretical foundation for the feasibility of observing FF states at finite temperature in a 2D system. It is expected that T_{BKT} is much lower than mean-field transition temperature (shown in the inset of Fig. 1 (a)), however, the finite momenta (shown in the inset of Fig. 1 (b)) evaluated at T_{BKT} of Cooper pairs are not destroyed by phase fluctuations. Fig. 1 (b) also shows $\rho_{xx} > \rho_{yy}$ due to the deformation of the equal thermodynamic potential along the y direction, instead of $\rho_{yy} > \rho_{xx} = 0$ for Fermi gases without SO coupling [17, 18].

With increasing in-plane Zeeman fields, the FF superfluids transit from gapped to gapless states [35, 38, 46–49] due to the strong distortion of quasi-particle excitations along the y direction. The gapless FF superfluids exhibit a Fermi surface in quasi-particle excitations as shown in Fig. 2(b). For a gapless superfluid, it is important to inquire whether the superfluids are stable. For instance, the famous gapless BP phase [50] with simple s-wave contact interactions was shown to be unstable with a negative superfluid density [51, 52]. In Fig. 1, we see that the superfluid densities for gapless states (the critical point of which is marked by a short line) are positive and T_{BKT} is finite, implying the superfluids are stable. Furthermore, there is an inflection point near the gapless transition point, corresponding to the minimum of the superfluid density and sound speeds. This point is exactly where the gap at zero momentum of quasi-particle excitations (shown in the inset of Fig. 1(c)) closes, indicating that phase fluctuations have dramatic effects at zero momentum, whereas the gapless surface emerges at nonzero momenta. Analogous to the anisotropic superfluid density tensor, the sound speeds shown in Fig. 1(c) are anisotropic along the x and y directions and even different along the positive and negative y directions. The anisotropy increases with the increasing Q_y with respect to h_x until the speed of sounds reaches the mini-

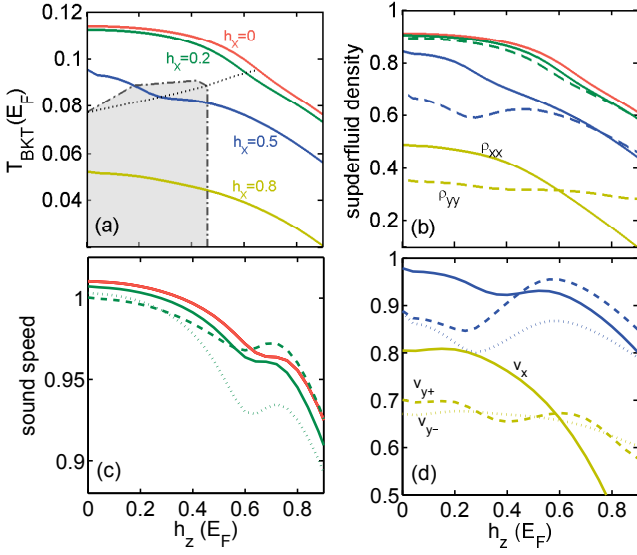


FIG. 3: (Color online) Plot of T_{BKT} (in (a)), superfluid density (in (b)) and sound speeds (in (c) and (d)) evaluated at T_{BKT} , as a function of h_z with h_x fixed. All states are FF superfluids except the one with $h_x = 0$. The black dotted line connects the topological transition points as h_x varies. The grey area surrounded by the dashed-dotted line maps out the gapless states region. The solid, dashed and dotted lines in (b), (c), and (d) label the corresponding superfluid densities and sound velocities as those in Fig. 1. Here $\alpha K_F = E_F$ and $E_b = 0.3E_F$.

imum where the gap at zero momentum is minimum. At $h_x = 0$, $v_x = v_{y+} = v_{y-}$ with the value close to $v_F/\sqrt{2}$ in the BCS limit.

In Fig. 1 (d), we plot the BKT temperature with respect to the binding energy E_b at fixed Zeeman fields. T_{BKT} is a monotonically increasing function of E_b , and approaches a constant value at large E_b that is independent of h_x , signalling the BCS-BEC crossover from BCS Cooper pairs to BEC tightly bound molecules. With increasing E_b , the emergence of an inflection point is accompanied by the critical transition point between gapped and gapless FF superfluids, arising from reduced finite momenta of Cooper pairs by E_b . Without Zeeman fields, no inflection appears because of the absence of transition between gapped and gapless superfluids.

In the presence of SO coupling and both in-plane and out-of-plane Zeeman fields, the topological FF superfluids [42–49] can emerge when $h_z > h_c$, across which the quasi-particle gap at zero momentum first closes and then reopens. There are two types of topological FF superfluids: topological FF superfluids and gapless topological FF superfluids, corresponding to gapped and gapless quasi-particle excitations respectively. In Fig. 3, we plot the changes of the BKT temperature T_{BKT} ((a)), the superfluid density ((b)), and the speeds of sound ((c) and (d)) with respect to h_z for fixed h_x . Since both Zeeman fields are detrimental to the Cooper pairing, T_{BKT}

is a monotonically decreasing function of Zeeman fields. However, given the existence of a gap close point at the transition boundary, similar to the case with only in-plane Zeeman field, it is expected that an inflection point can emerge at this point. Interestingly, Fig. 3 shows that this inflectional behavior is hardly noticed for small h_x (red and green lines respectively for $h_x = 0$ and $h_x = 0.2$) for topological FF superfluids and becomes manifest with increasing h_x , especially for gapless superfluids (blue line for $h_x = 0.5$). Physically, this phenomenon results from the enlarged density of states at zero momentum for gapless superfluids as visualized in Fig. 2. Similar to the case with pure h_x , the sound speeds shown in Fig. 3(c) and (d) with respect to h_z have the minimum at the topological phase transition boundary. Furthermore, the sound speeds along the x direction fall quicker than along the y direction with increasing h_z , leading to the reverse of superfluid densities that $\rho_{xx} < \rho_{yy}$ in the topological region at large h_z . The reason is the symmetry restoration of the Fermi surface at large h_z , where Q_y begins decreasing.

In Fig. 3(a), the dotted line represents T_{BKT} at the topological transition points as h_x varies, showing that T_{BKT} decreases with increasing h_x while the critical h_z decreases. This indicates that the existence of h_x cannot enhance the BKT temperature for the observation of topological superfluids. The grey region surrounded by the dashed-dotted line is where the gapless topological superfluids can be observed. Compared to the 3D case where the gapless topological superfluids are dominant [46], this region is much smaller.

Below the BKT temperature, the superfluids are affluent with V-AV pairs, which can be obtained by solving $\nabla \times \mathbf{v}_s = 2\pi \sum_i n_i \delta(\mathbf{r} - \mathbf{r}_i)$ and the minimization of S_{eff}^v : $\rho_{xx} \partial_x^2 \theta_v + \rho_{yy} \partial_y^2 \theta_v = 0$. Here $\mathbf{v}_s = \nabla \theta_v(\mathbf{r})$, $n_i = \pm 1$ represents a vortex or antivortex localized at \mathbf{r}_i . For a single vortex, $\theta_v = \arctan(\rho^2 y/x)$ with $\rho = (\rho_{xx}/\rho_{yy})^{1/4}$. For a V-AV pair located at $(\pm x_0, 0)$, $\theta_v = \arctan[2\bar{x}_0 \bar{y}/(\bar{x}_0^2 - \bar{x}^2 - \bar{y}^2)]$ with $\bar{x} = x/\rho$, $\bar{y} = y/\rho$, and $\bar{a} = a/\rho$. Interestingly, the anisotropic superfluid densities induced by the finite momentum pairing results in anisotropic V-AV pairs (See supplementary materials) in contrast to isotropic ones in normal BCS superfluids for Rashba-type spin-orbit coupled Fermi gases [14–16, 54]. Anisotropic V-AV pairs have also been discussed recently where the anisotropy is caused by the anisotropic SO coupling [53], instead of FF pairing here.

To summary, we investigate the BKT phase transition for a 2D SO coupled Fermi gas subject to Zeeman fields and find finite BKT temperatures for both gapped and gapless FF superfluids in sharp contrast to the case without SO coupling, where it is zero due to the vanishing transverse superfluid density. Our findings demonstrate the feasibility for the experimental observation of FF superfluids (gapped or gapless, topological or non-topological) and the associated topological excita-

tions (e.g., Majorana fermions) in a 2D spin-orbit coupled Fermi gas at finite temperature.

Acknowledgement: This work is supported by ARO (W911NF-12-1-0334), AFOSR (FA9550-11-1-0313 and FA9550-13-1-0045), and NSF-PHY (1249293). We thank Texas Advanced Computing Center (TACC), where our numerical simulations were performed.

* Corresponding Author, Email: chuanwei.zhang@utdallas.edu

- [1] P. Fulde and R. A. Ferrell, *Phys. Rev.* **135**, A550 (1964).
- [2] A. I. Larkin and Yu. N. Ovchinnikov, *Zh. Eksp. Teor. Fiz.* **47**, 1136 (1964) [*Sov. Phys. JETP* **20**, 762 (1965)].
- [3] H. A. Radovan, N. A. Fortune, T. P. Murphy, S. T. Hannahs, E. C. Palm, S. W. Tozer, and D. Hall, *Nature* **425**, 51 (2003).
- [4] A. Bianchi, R. Movshovich, C. Capan, P. G. Pagliuso, and J. L. Sarrao, *Phys. Rev. Lett.* **91**, 187004 (2003).
- [5] M. Kenzelmann, Th. Strässle, C. Niedermayer, M. Sigrist, B. Padmanabhan, M. Zolliker, A. D. Bianchi, R. Movshovich, E. D. Bauer, J. L. Sarrao, and J. D. Thompson, *Science* **321** 1652 (2008).
- [6] S. Uji, T. Terashima, M. Nishimura, Y. Takahide, T. Konoike, K. Enomoto, H. Cui, H. Kobayashi, A. Kobayashi, H. Tanaka, M. Tokumoto, E. S. Choi, T. Tokumoto, D. Graf, and J. S. Brooks, *Phys. Rev. Lett.* **97**, 157001 (2006).
- [7] L. Li, C. Richter, J. Mannhart, and R. C. Ashoori, *Nature* **7**, 762 (2011).
- [8] Y. Liao, A. S. C. Rittner, T. Paprotta, W. Li, G. B. Partridge, R. G. Hulet, S. K. Baur, and E. J. Mueller, *Nature* **467**, 567 (2010).
- [9] D. E. Sheehy and L. Radzihovsky, *Phys. Rev. Lett.* **96**, 060401 (2006).
- [10] M. M. Parish, S. K. Baur, E. J. Mueller, and D. A. Huse, *Phys. Rev. Lett.* **99**, 250403 (2007).
- [11] T. K. Koponen, T. Paananen, J.-P. Martikainen, M. R. Bakhtiari, P. Törmä, *New Journal of Physics* **10**, 045104 (2008).
- [12] V. L. Berezinskii, *Sov. Phys. JETP* **32**, 493 (1971).
- [13] J. M. Kosterlitz and D. Thouless, *J. Phys. C* **5**, L124 (1972); **6**, 1181 (1973).
- [14] S. S. Botelho and C. A. R. Sá de Melo, *Phys. Rev. Lett.* **96**, 040404 (2006).
- [15] L. He and X. -G. Huang, *Phys. Rev. Lett.* **108**, 145302 (2012).
- [16] M. Gong, G. Chen, S. Jia, and C. Zhang, *Phys. Rev. Lett.* **109**, 105302 (2012).
- [17] L. Radzihovsky and A. Vishwanath, *Phys. Rev. Lett.* **103**, 010404 (2009).
- [18] S. Yin, J. -P. Martikainen, and P. Törmä, *Phys. Rev. B* **89**, 014507 (2014).
- [19] Y. -J. Lin, K. Jiménez-García, and I. B. Spielman, *Nature (London)* **471**, 83 (2011).
- [20] P. Wang, Z. -Q. Yu, Z. Fu, J. Miao, L. Huang, S. Chai, H. Zhai, and J. Zhang, *Phys. Rev. Lett.* **109**, 095301 (2012).
- [21] L. W. Cheuk, A. T. Sommer, Z. Hadzibabic, T. Yefsah, W. S. Bakr, and M. W. Zwierlein, *Phys. Rev. Lett.* **109**, 095302 (2012).
- [22] J. -Y. Zhang, S. -C. Ji, Z. Chen, L. Zhang, Z. -D. Du, B. Yan, G. -S. Pan, B. Zhao, Y. -J. Deng, H. Zhai, S. Chen, and J. -W. Pan, *Phys. Rev. Lett.* **109**, 115301 (2012).
- [23] C. Qu, C. Hamner, M. Gong, C. Zhang, and P. Engels, *Phys. Rev. A* **88**, 021604(R) (2013).
- [24] R. A. Williams, M. C. Beeler, L. J. LeBlanc, K. Jiménez-García, and I. B. Spielman, *Phys. Rev. Lett.* **111**, 095301 (2013).
- [25] V. Galitski and I. B. Spielman, *Nature (London)* **494**, 49 (2013).
- [26] C. Zhang, S. Tewari, R. M. Lutchyn, and S. Das Sarma, *Phys. Rev. Lett.* **101**, 160401 (2008).
- [27] M. Sato, Y. Takahashi, and S. Fujimoto, *Phys. Rev. Lett.* **103**, 020401 (2009).
- [28] S. -L. Zhu, L. -B. Shao, Z. D. Wang, and L. -M. Duan, *Phys. Rev. Lett.* **106**, 100404 (2011).
- [29] L. Jiang, T. Kitagawa, J. Alicea, A. R. Akhmerov, D. Pekker, G. Refael, J. I. Cirac, E. Demler, M. D. Lukin, and P. Zoller, *Phys. Rev. Lett.* **106**, 220402 (2011).
- [30] L.-J. Lang, X. Cai, and S. Chen, *Phys. Rev. Lett.* **108**, 220401 (2012).
- [31] X. Zhou, Y. Li, Z. Cai, and Congjun Wu, *J. Phys. B: At. Mol. Opt. Phys.* **46**, 134001 (2013).
- [32] X. -J. Liu, K. T. Law, and T. K. Ng, *Phys. Rev. Lett.* **112**, 086401 (2014).
- [33] A. Kitaev, *Ann. Phys. (N. Y.)* **303**, 2 (2003).
- [34] Z. Zheng, M. Gong, X. Zou, C. Zhang, and G. Guo, *Phys. Rev. A* **87**, 031602(R) (2013).
- [35] F. Wu, G.-C. Guo, W. Zhang, and W. Yi, *Phys. Rev. Lett.* **110**, 110401 (2013).
- [36] X.-J. Liu and H. Hu, *Phys. Rev. A* **87**, 051608(R) (2013).
- [37] Z. Fu, L. Huang, Z. Meng, P. Wang, X.-J. Liu, H. Pu, H. Hu, and J. Zhang, *Phys. Rev. A* **87**, 053619 (2013).
- [38] L. Dong, L. Jiang, and H. Pu, *New Journal of Physics* **15**, 075014 (2013).
- [39] H. Hui and X.-J. Liu, *New Journal of Physics* **15**, 093037 (2013).
- [40] M. Iskin, *Phys. Rev. A* **88**, 013631 (2013).
- [41] Y. Xu, C. Qu, M. Gong, and C. Zhang, *Phys. Rev. A* **89**, 013607 (2014).
- [42] C. Qu, Z. Zheng, M. Gong, Y. Xu, L. Mao, X. Zou, G. Guo, and C. Zhang, *Nature Communications* **4**, 2710 (2013).
- [43] W. Zhang and W. Yi, *Nature Communications* **4**, 2711 (2013).
- [44] X. -J. Liu and H. Hu, *Phys. Rev. A* **88**, 023622 (2013).
- [45] C. Chen, *Phys. Rev. Lett.* **111**, 235302 (2013).
- [46] Y. Xu, R.-L. Chu, and C. Zhang, *Phys. Rev. Lett.* **112**, 136402 (2014).
- [47] C. F. Chan and M. Gong, *Phys. Rev. B* **89**, 174501 (2014).
- [48] Y. Cao, S.-H. Zou, X.-J. Liu, S. Yi, G.-L. Long, and H. Hu, *arXiv:1402.6832*.
- [49] H. Hu, L. Dong, Y. Cao, H. Pu, and X. -J. Liu, *arXiv:1404.2442*.
- [50] W. V. Liu and F. Wilczek, *Phys. Rev. Lett.* **90**, 047002 (2003).
- [51] S.-T. Wu and S. Yip, *Phys. Rev. A* **67**, 053603 (2003).
- [52] M. M. Forbes, E. Gubankova, W. V. Liu, and F. Wilczek, *Phys. Rev. Lett.* **94**, 017001 (2005).
- [53] J. P. A. Devreese, J. Tempere, and C. A. R. Sá de Melo, *arXiv:1403.5780*.
- [54] K. Zhou and Z. Zhang, *Phys. Rev. Lett.* **108**, 025301 (2012).

SUPPLEMENTARY MATERIALS

In the main text we present various physical quantities including the BKT temperature, superfluid density tensor, and speed of sound for a spin-orbit coupled Fermi gas subject to both in-plane and out-of-plane Zeeman fields. Here we provide more detailed calculation information in Sec. S-1 and S-2 and plot anisotropic V-AV structures in Sec. S-3.

S-1. DERIVATION OF SUPERFLUID DENSITY TENSOR AND SOUND SPEED

In quantum field theory, the partition function can be written as $Z = \text{Tr}(e^{-\beta H}) = \int D(\bar{\psi}, \psi) e^{-S_{eff}[\bar{\psi}, \psi]}$ with $\beta = 1/T$ at the temperature T . The effective action is

$$S_{eff}[\bar{\psi}, \psi] = \int_0^\beta d\tau \left(\int d\mathbf{r} \sum_\sigma \bar{\psi}_\sigma(\mathbf{r}, \tau) \partial_\tau \psi_\sigma(\mathbf{r}, \tau) + H(\bar{\psi}, \psi) \right), \quad (6)$$

where $\int d\tau$ is an integral over the imaginary time τ and $H(\bar{\psi}, \psi)$ is obtained by replacing $\hat{\Psi}_\sigma^\dagger$ and $\hat{\Psi}_\sigma$ with Grassman field number $\bar{\psi}_\sigma$ and ψ_σ . We can transform the quartic interaction term to quadratic one by Hubbard-Stratonovich transformation, where the order parameter $\Delta(\mathbf{r}, \tau)$ is defined. By integrating out fermion fields, the partition function becomes $Z = \int D(\bar{\Delta}, \Delta) e^{-S_{eff}[\bar{\Delta}, \Delta]}$, where the effective action can be written as

$$S_{eff}[\bar{\Delta}, \Delta] = \int_0^\beta d\tau \int d\mathbf{r} \left(\frac{|\Delta|^2}{U} \right) - \frac{1}{2} \ln \det G^{-1}. \quad (7)$$

Here the inverse single particle Green function $G^{-1} = -\partial_\tau - H_B$ in the Nambu-Gor'kov representation with 4×4 Bogoliubov-de Gennes (BdG) Hamiltonian

$$H_B = \begin{pmatrix} H_s(\hat{\mathbf{p}}) & \Delta(\mathbf{r}, \tau) \\ \Delta(\mathbf{r}, \tau) & -\sigma_y H_s(\hat{\mathbf{p}})^* \sigma_y \end{pmatrix}. \quad (8)$$

Assume that a mean-field solution has the FF form $\Delta(\mathbf{r}, \tau)_0 = e^{iQ_y y} \Delta_0$ with the space independent Δ_0 given that the in-plane Zeeman field deforms the Fermi surface along the y direction, leading to finite momentum pairing along that direction [1]. Through Fourier transformation and the summation of Matsubara frequency, this form of $\Delta(\mathbf{r}, \tau)$ yields mean-field thermodynamical potential [2, 3].

To study the effects of phase fluctuations, we assume $\Delta(\mathbf{r}) = \Delta_0 e^{iQ_y y + i\theta(\tau, \mathbf{r})}$ with phase fluctuations field $\theta(\tau, \mathbf{r})$ around the saddle point. The unitary transformed inverse Green function becomes

$$G^{-1} = G_0^{-1} + \Sigma, \quad (9)$$

via the unitary operator

$$U = \begin{pmatrix} e^{i(\theta + Q_y y)} & 0 \\ 0 & e^{-i(\theta + Q_y y)} \end{pmatrix}. \quad (10)$$

Here G_0^{-1} represents the mean-field part and

$$\begin{aligned} \Sigma = & [i\partial_\tau \theta / 2 + \hbar^2 Q_y \partial_y \theta / 4m + \hbar^2 (\nabla \theta)^2 / 8m] \sigma_z \otimes \sigma_0 + \hbar \nabla \theta \cdot \hat{\mathbf{p}} / 2m \\ & - i\hbar^2 \nabla^2 \theta / 4m + \alpha \hbar \partial_x \theta / 2 (\sigma_0 \otimes \sigma_y) - \alpha \hbar \partial_y \theta / 2 (\sigma_0 \otimes \sigma_x), \end{aligned} \quad (11)$$

the self-energy contributed by phase fluctuations. Substituting Eq. 9 to Eq. 7 leads to the effective action

$$S_{eff} = S_{eff}^0 + S_{eff}^{fluc}, \quad (12)$$

where $S_{eff}^{fluc} = \text{tr} \sum_{n=1}^\infty (G_0 \Sigma)^n / 2n$ represents phase fluctuation contributions. Expanding it to the second order yields

$$\begin{aligned} S_{eff}^{fluc} &= \frac{1}{2} \text{tr}_4 G_0 \Sigma + \frac{1}{4} \text{tr}_4 (G_0 \Sigma G_0 \Sigma) \\ &= \frac{1}{2} \int d\mathbf{r} \int d\tau [J_{xx} (\partial_x \theta)^2 + J_{yy} (\partial_y \theta)^2 + J_{xy} \partial_x \theta \partial_y \theta + iJ_{\tau y} \partial_\tau \theta \partial_y \theta + iJ_{\tau x} \partial_\tau \theta \partial_x \theta + P(\partial_\tau \theta)^2 - iA \partial_\tau \theta] \end{aligned} \quad (13)$$

where

$$J_{xx} = \frac{\hbar^2}{4m}n + \frac{1}{8\beta(2\pi)^2} \int d\mathbf{k} \sum_{\omega_n} \left(\hbar^2 \alpha^2 f_{44} + \frac{\hbar^2}{m^2} f_{22} k_x^2 + \frac{2\hbar^2 \alpha}{m} f_{24} k_x \right) \quad (14)$$

$$J_{yy} = \frac{\hbar^2}{4m}n + \frac{1}{8\beta(2\pi)^2} \int d\mathbf{k} \sum_{\omega_n} \left(\frac{\hbar^4}{4m^2} f_{11} Q_y^2 - \frac{\hbar^3 \alpha}{m} f_{15} Q_y + \hbar^2 \alpha^2 f_{55} + \frac{\hbar^3}{m^2} f_{12} Q_y k_y + \frac{\hbar^2}{m^2} f_{22} k_y^2 - \frac{2\hbar^2 \alpha}{m} f_{25} k_y \right) \quad (15)$$

$$J_{xy} = \frac{1}{4\beta(2\pi)^2} \int d\mathbf{k} \sum_{\omega_n} \left(\frac{\hbar^3 \alpha}{2m} f_{14} Q_y - \hbar^2 \alpha^2 f_{45} + \frac{\hbar^3}{2m^2} f_{12} Q_y k_x + \frac{\hbar^2}{m^2} f_{22} k_x k_y + \frac{\hbar^2 \alpha}{m} f_{24} k_y - \frac{\hbar^2 \alpha}{m} f_{25} k_x \right) \quad (16)$$

$$P = -\frac{1}{8} \frac{1}{\beta(2\pi)^2} \int d\mathbf{k} \sum_{\omega_n} f_{11} \quad (17)$$

$$A = n \quad (18)$$

$$J_{\tau y} = \frac{1}{8\beta(2\pi)^2} \int d\mathbf{k} \sum_{\omega_n} \left(\frac{\hbar^2}{m} f_{11} Q_y - 2\hbar \alpha f_{15} + \frac{2\hbar}{m} f_{12} k_y \right) \quad (19)$$

$$J_{\tau x} = \frac{1}{4\beta(2\pi)^2} \int d\mathbf{k} \sum_{\omega_n} \left(\hbar \alpha f_{14} + \frac{\hbar}{m} f_{12} k_x \right) \quad (20)$$

and

$$\begin{aligned} f_{11} &= \text{tr}_4 G_0(-i\omega_n, \mathbf{k})(\sigma_z \otimes \sigma_0) G_0(-i\omega_n, \mathbf{k})(\sigma_z \otimes \sigma_0) \\ f_{14} &= \text{tr}_4 G_0(-i\omega_n, \mathbf{k}) \sigma_0 \otimes \sigma_y G_0(-i\omega_n, \mathbf{k}) \sigma_z \otimes \sigma_0 \\ f_{15} &= \text{tr}_4 G_0(-i\omega_n, \mathbf{k}) \sigma_0 \otimes \sigma_x G_0(-i\omega_n, \mathbf{k}) \sigma_z \otimes \sigma_0 \\ f_{44} &= \text{tr}_4 G_0(-i\omega_n, \mathbf{k}) \sigma_0 \otimes \sigma_y G_0(-i\omega_n, \mathbf{k}) \sigma_0 \otimes \sigma_y \\ f_{45} &= \text{tr}_4 G_0(-i\omega_n, \mathbf{k}) \sigma_0 \otimes \sigma_x G_0(-i\omega_n, \mathbf{k}) \sigma_0 \otimes \sigma_y \\ f_{55} &= \text{tr}_4 G_0(-i\omega_n, \mathbf{k}) \sigma_0 \otimes \sigma_x G_0(-i\omega_n, \mathbf{k}) \sigma_0 \otimes \sigma_x \\ f_{12} &= \text{tr}_4 G_0(-i\omega_n, \mathbf{k}) G_0(-i\omega_n, \mathbf{k}) \sigma_z \otimes \sigma_0 \\ f_{22} &= \text{tr}_4 G_0(-i\omega_n, \mathbf{k}) G_0(-i\omega_n, \mathbf{k}) \\ f_{24} &= \text{tr}_4 G_0(-i\omega_n, \mathbf{k}) \sigma_0 \otimes \sigma_y G_0(-i\omega_n, \mathbf{k}) \\ f_{25} &= \text{tr}_4 G_0(-i\omega_n, \mathbf{k}) \sigma_0 \otimes \sigma_x G_0(-i\omega_n, \mathbf{k}) \end{aligned}$$

Here $G_0(-i\omega_n, \mathbf{k})$ is the Fourier transformation of $G_0(\mathbf{r}, \tau)$ with Matsubara frequency $\omega_n = (2n+1)\pi/\beta$; tr_4 represents the trace calculation for a 4×4 matrix. Note that we calculate the summation over Matsubara frequency numerically due to the absence of the analytical expression of G_0 .

Our numerical results show that $J_{xy} = 0$ and $J_{\tau x} = 0$ while $J_{\tau y} \neq 0$ for FF superfluids, which is reasonable considering that the symmetry of the quasi-particle excitations along the y direction is broken while that along the x direction is kept. In the absence of Zeeman fields, these parameters can be analytically written as

$$\begin{aligned} J_{xx} &= J_{yy} \\ &= \frac{\hbar^2}{4m} \left[n - \frac{1}{V} \sum_{\mathbf{k}} \sum_{L=\pm} \left(\frac{\alpha^2 m}{4E_L} \tanh(\beta E_L/2) \left(1 + L \frac{\epsilon_{\mathbf{k}}^2}{|\alpha|k|\xi_{\mathbf{k}}|} \right) + \frac{\beta m}{8\hbar^2} \left(\alpha - L \frac{\hbar \xi_{\mathbf{k}} k}{m|\xi_{\mathbf{k}}|} \right)^2 \text{sech}(\beta E_L/2)^2 \right) \right] \end{aligned} \quad (21)$$

$$P = \frac{1}{8} \frac{1}{V} \sum_{\mathbf{k}} \sum_{L=\pm} \left[\frac{\beta}{2} \text{sech}(\beta E_L/2)^2 \left(\frac{\xi_{\mathbf{k}}}{E_L} \right)^2 \left(1 + L \frac{|\alpha|k}{|\xi_{\mathbf{k}}|} \right)^2 + \frac{1}{E_L} \tanh(\beta E_L/2) \left(\frac{\Delta}{E_L} \right)^2 \right] \quad (22)$$

$$Q = n \quad (23)$$

and $J_{xy} = J_{\tau y} = J_{\tau x} = 0$. Here the quasi-particle excitation spectrum is

$$E_L = \xi_{\mathbf{k}}^2 + \alpha^2 k^2 + \Delta^2 + 2Lk|\alpha \xi_{\mathbf{k}}| \quad (24)$$

with $\xi_{\mathbf{k}} = \hbar^2 k^2 / 2m - \mu$. These expressions are exactly the same as previous results [4]. For the FF superfluids, $Q_y \neq 0$, leading to $J_{xx} \neq J_{yy}$ corresponding to anisotropic superfluid densities.

To obtain the low excitation spectrum, we write the effective action in Fourier space

$$S_{eff}^{fluc} = \frac{1}{2} \sum_{\mathbf{k}n} (J_x k_x^2 + J_y k_y^2 - J_{\tau y} E_{sw}(\mathbf{k}) k_y - P E_{sw}(\mathbf{k})^2) \theta(n, \mathbf{k}) \theta(-n, -\mathbf{k}) \quad (25)$$

where $\theta(n, \mathbf{k})$ is the Fourier transformation of $\theta(\mathbf{r}, \tau)$; $i\omega_n$ has been taken analytically to $E_{sw}(\mathbf{k} + i0^+)$. The low excitation energy spectrum can be obtained by

$$P E_{sw}(\mathbf{k})^2 + J_{\tau y} k_y E_{sw}(\mathbf{k}) - J_x k_x^2 - J_y k_y^2 = 0 \quad (26)$$

which leads to the dispersion

$$E_{sw}(\mathbf{k}) = \frac{-J_{\tau y} k_y + \sqrt{J_{\tau y}^2 k_y^2 + 4P(J_x k_x^2 + J_y k_y^2)}}{2P} \quad (27)$$

Clearly, the dispersion along each direction is linear around $k = 0$, with the slope (i.e. sound speeds) written as

$$v_x = \sqrt{\frac{J_x}{P}} \quad (28)$$

$$v_{y+} = \frac{-J_{\tau y} + \sqrt{J_{\tau y}^2 + 4PJ_y}}{2P} \quad (29)$$

$$v_{y-} = \frac{J_{\tau y} + \sqrt{J_{\tau y}^2 + 4PJ_y}}{2P} \quad (30)$$

In normal superfluids where $J_{\tau y} = 0$ and $J_x = J_y$, the speeds of sound are isotropic. However, in FF superfluids where $J_{\tau y} \neq 0$ and $J_x \neq J_y$, they are anisotropic and even different along the positive and negative y directions. It is important to note that anisotropic sound speeds also happen in anisotropic systems such as equal Rashba-Dresshaus spin-orbit coupled Fermi gases [5] where $J_x \neq J_y$, but in that system $J_{\tau y} = 0$, implying that they are the same along the positive and negative y directions.

The integration of spin-wave part yields

$$S_{eff}^{sw} = \sum_{\mathbf{k}} \ln(1 - e^{-\beta E_{sw}(\mathbf{k})}) \quad (31)$$

In the presence of spin-wave excitations, the generalized saddle point equation and particle number equation become $\partial\Omega^0/\partial\Delta_0 = 0$, $\partial\Omega/\partial Q_y = 0$, and $\partial\Omega/\partial\mu = -n$.

S-2. GENERALIZED KOSTERLITZ-THOULESS RELATION

For FF superfluids with anisotropic superfluid densities, the BK relation [6, 7] corresponding to isotropic superfluid densities should be generalized. We consider a free vortex $\theta_v = \arctan(\rho^2 y/x)$ emerging at the temperature T in a FF superfluid, the free-energy change of the system is

$$F = U_v - TS_v, \quad (32)$$

where U_v is the energy of the vortex in a system of size R

$$\begin{aligned} U_v &= \int d\mathbf{r} [J_{xx}(\partial_x \theta_v)^2 + J_{yy}(\partial_y \theta_v)^2] \\ &= \pi \sqrt{J_{xx} J_{yy}} \ln(R/a) \end{aligned} \quad (33)$$

with the size of the vortex core a . The entropy of the vortex is

$$S_v = 2\ln\left(\frac{R}{a}\right) \quad (34)$$

because the number of configurations that a vortex localizes in a system is $(R/a)^2$. Here we set $k_b = 1$. It turns out that a single vortex can be thermally excited when $F = 0$, leading to the BKT temperature

$$T = \frac{\pi}{2} \sqrt{J_{xx} J_{yy}} \quad (35)$$

This is the generalized KT relation [5], which becomes KT relation when $J_{xx} = J_{yy}$.

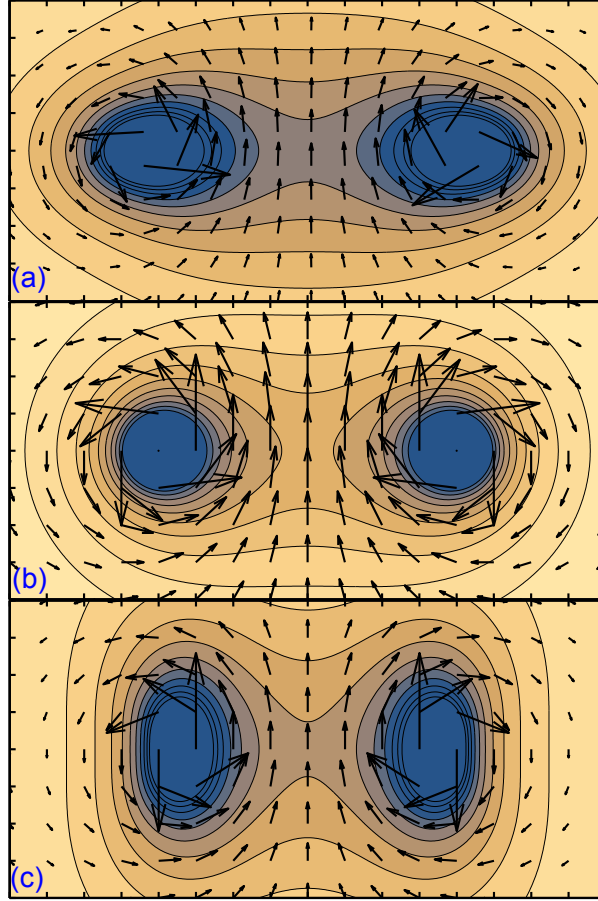


FIG. 4: (Color online) Vortex-antivortex structure for topological superfluids corresponding to $\rho_{xx} > \rho_{yy}$ in (a) with $h_z = 0.04E_F$, $\rho_{xx} = \rho_{yy}$ in (b) with $h_z = 0.6E_F$, and $\rho_{xx} < \rho_{yy}$ in (c) with $h_z = 0.8E_F$, evaluated around T_{BKT} . Here $\alpha K_F = E_F$, $E_b = 0.3E_F$, and $h_x = 0.8E_F$.

S-3. VORTEX-ANTIVORTEX VELOCITY FIELD STRUCTURE

In the main text, we have shown that anisotropic V-AV pairs emerges across the BKT temperature. The anisotropy originates from the phase field depending on the ratio of superfluid densities along different directions. Here, to visualize V-AV pairs, we plot their velocity fields in Fig. 4. It is clearly shown that there are three distinct vortex cores: elliptical with the major axis along the x direction in (a), circular in (b), and elliptical with the major axis along the y direction in (c), corresponding to $\rho_{xx} > \rho_{yy}$, $\rho_{xx} = \rho_{yy}$, and $\rho_{xx} < \rho_{yy}$ respectively. We note that although V-AV pairs have circular structure in (b), the same as traditional BCS superfluids, the superfluids have Cooper pairs with finite center-of-mass momenta.

* Corresponding Author, Email: chuanwei.zhang@utdallas.edu

- [1] Y. Xu, C. Qu, M. Gong, and C. Zhang, Phys. Rev. A **89**, 013607 (2014).
- [2] Z. Zheng, M. Gong, X. Zou, C. Zhang, and G. Guo, Phys. Rev. A **87**, 031602(R) (2013).
- [3] Y. Xu, R.-L. Chu, and C. Zhang, Phys. Rev. Lett. **112**, 136402 (2014).
- [4] M. Gong, G. Chen, S. Jia, and C. Zhang, Phys. Rev. Lett. **109**, 105302 (2012).
- [5] J. P.A. Devreese, J. Tempere, C. A.R. Sá de Melo, arXiv:1403.5780.
- [6] V. L. Berezinskii, Sov. Phys. JETP **32**, 493 (1971).
- [7] J. M. Kosterlitz and D. Thouless, J. Phys. C **5**, L124 (1972); **6**, 1181 (1973).